Journal Pre-proof

Highly diverse diazotrophs drive high N_2 fixation rates in a shallow submarine hydrothermal system

Mingming Chen , Yufang Li , Kai Tang , Anyi Hu , Wei Fan , Deli Wang , Chen-Tung Arthur Chen , Yao Zhang

PII: S2667-3258(23)00271-6
DOI: https://doi.org/10.1016/j.fmre.2023.07.009
Reference: FMRE 612

To appear in: *Fundamental Research*

Received date: 10 October 2022
Revised date: 19 June 2023
Accepted date: 7 July 2023

Please cite this article as: Mingming Chen , Yufang Li , Kai Tang , Anyi Hu , Wei Fan , Deli Wang , Chen-Tung Arthur Chen , Yao Zhang , Highly diverse diazotrophs drive high N_2 fixation rates in a shallow submarine hydrothermal system, *Fundamental Research* (2023), doi: https://doi.org/10.1016/j.fmre.2023.07.009

Highly diverse diazotrophs drive high N_2 fixation rates in a shallow submarine hydrothermal system

Mingming Chen[a,1], Yufang Li[b,1], Kai Tang[a], Anyi Hu[c,d], Wei Fan[e], Deli Wang[a], Chen-Tung Arthur Chen[f], Yao Zhang[a,*]

[a]*State Key Laboratory of Marine Environmental Science, College of Ocean and Earth Sciences, Xiamen University, Xiamen 361102, China*

[b]*Fisheries College, Jimei University, Xiamen 361021, China*

[c]*CAS Key Laboratory of Urban pollutant Conversion & Fujian Key Laboratory of Watershed Ecology, Institute of Urban Environment, Chinese Academy of Sciences, Xiamen 361021, China*

[d]*University of Chinese Academy of Sciences, Beijing 100049, China*

[e]*Ocean College, Zhejiang University, Zhoushan 316022, China*

[f]*Department of Oceanography, Sun Yat-Sen University (Taiwan), Taiwan 080471, China*

[*]*Corresponding author: yaozhang@xmu.edu.cn (Y. Zhang).*

[1]*These authors contributed equally to this work*

ABSTRACT

Dinitrogen (N_2) fixation provides nitrogen sources supporting active chemoautotrophic processes in submarine hydrothermal systems. Here, the diazotrophic phylogenetic diversity and N_2 fixation profile were investigated in depth along a sharp biogeochemical gradient from the hydrothermal vents to ambient seawater in a shallow submarine hydrothermal system (SHS) off Kueishantao Islet, Taiwan. Diazotrophic community compositions in the SHS covered all four known *nifH* clusters (I, II, III, and IV) and contained both characteristics of diazotrophic communities in deep-sea hydrothermal systems and terrestrial geothermal systems. The seawater around the vents was primarily dominated by *nifH* phylotypes affiliated with chemolithotrophic sulfur-oxidizing and iron-reducing bacteria. In contrast, in the seawater directly above the hydrothermal vents, the *nifH* community markedly contained diverse heterotrophic bacteria. The analysis, which focused on amino acid composition, protein spatial structure, and the possible co-occurrence of alternative nitrogenases in the presence of molybdenum-nitrogenase, further revealed that diazotrophic nitrogenase found around the hydrothermal vents exhibits potential molecular adaptations to high temperature, low pH, and sulfur-rich conditions. The relatively low N_2 fixation rates (NFRs) were observed around the vents, where high concentrations of inorganic nitrogen compounds were present. However, notably, high NFRs were detected in seawater directly above the hydrothermal vents, which were 2–5 times higher than those at the reference site. The abundant iron, along with the depletion of nitrogen nutrients potentially resulting from nitrogen assimilation and

loss processes, may have led to a high iron:nitrogen ratio, inducing the observed high NFRs. The co-occurrence of diverse *nifH*-containing heterotrophic bacteria and high NFRs suggests that these heterotrophs may play a major role in N_2 fixation in this environment. This study suggests that the SHSs may be potential hotspots for marine N_2 fixation, contributing significantly to the global ocean's N_2 fixation budget and warranting further investigation.

Keywords: shallow submarine hydrothermal system; N_2 fixation; heterotrophic diazotrophs; biogeochemical gradient; sulfur and iron metabolism

1. Introduction

Submarine hydrothermal systems are among the most extreme and primeval environments on the earth. In these niches, geothermal energy is transferred into chemical energy in the form of reduced inorganic compounds like sulfureted hydrogen, hydrogen, methane (CH_4), manganous ion (Mn^{2+}), ferrous ion (Fe^{2+}), and carbon monoxide, and fuels for carbon fixation of chemolithotrophic microorganisms [1,2]. High productivity requires sufficient support from nitrogen sources. In inorganic nitrogen-rich hydrothermal vents, the assimilation of inorganic nitrogen can be an important nitrogen source. For example, a previous study in the Rose Garden vent field showed the removal of nitrate (NO_3^-) and accumulation of ammonium (NH_4^+) in the hydrothermal vent, implying active uptake and reduction of NO_3^- for meeting vent animals' requirements of nitrogen [3]. Active assimilation and oxidation of NH_4^+ were also reported in the hydrothermal plume at Endeavour Segment, Juan de Fuca Ridge [4]. However, inorganic nitrogen concentrations sharply attenuated in ambient seawater off the hydrothermal vents [3,4]. Besides, low concentrations of NH_4^+, NO_3^-, and nitrite (NO_2^-), or the animals' nitrogen isotope ratios ($\delta^{15}N$) lower than that of deep-sea organic nitrogen but resembling those of deep oceanic N_2, were also found in some hydrothermal vents [5,6]. Taken together we may hypothesize that biological N_2 fixation could occur actively in hydrothermal ecosystems.

Phylogenetic diversity of the nitrogenase iron protein gene (*nifH*), which is a typical molecular marker to determine the potential of biological N_2 fixation [7,8], has been explored in some typical deep-sea hydrothermal systems (DHSs) on the Juan de Fuca Ridge, the Southwest Indian Ridge, and the South Atlantic Middle Ridge. The results indicate the existence of diverse diazotrophs, including heterotrophic proteobacteria, archaea, and sulfate reducers, in these DHSs [5,9,10,11]. A methanogenic archaeal strain FS406-22, which was capable of performing N_2 fixation at up to 92 °C (the currently known upper temperature limit of biological N_2 fixation), was isolated from deep-sea hydrothermal vent fluid [6]. Except for this case, however, the activity of diazotrophs in submarine hydrothermal systems has hardly been confirmed. A big mismatch between gene and transcript abundance of *nifH* in hydrothermal vent fluids has been reported in a previous study [12]. Therefore, *in situ* measurements of N_2 fixation rates (NFRs) combined with the phylogenetic diversity

of nitrogen-fixers can verify the biological N_2 fixation in submarine hydrothermal systems.

Marine biological N_2 fixation is regulated by various factors, mainly temperature, concentrations of oxygen gas (O_2), carbon dioxide (CO_2), fixed nitrogen, phosphorus, and iron (Fe), as well as dynamical processes [13]. Coincidentally, most of these factors show steep spatial gradient variations in hydrothermal systems [1], implying a complex and drastic fluctuation of N_2 fixation there. Although extreme temperature (up to >350 °C) in hydrothermal vents has been thought to be a huge obstacle for N_2 fixation by diazotrophs, N_2 fixation has been demonstrated in hyperthermophilic and thermophilic diazotrophs from high-temperature submarine and terrestrial geothermal systems (TGSs) [6,14,15]. Besides, ample sulfur in hydrothermal vents also has a potential influence on diazotrophic community structure by stimulating sulfur metabolism-related diazotrophs. Previous studies have reported abundant sulfate-reducing N_2-fixers in DHSs [5,11]. Moreover, the rich sulfide in hydrothermal systems would coprecipitate with bioavailable molybdate (Mo), which is the key element in Mo-nitrogenase (the most common form of nitrogenase), into sedimentary sulfides and organic matters, providing favorable conditions for N_2 fixation by alternative vanadium (V)- and Fe-only nitrogenases and impacting local N cycle [16]. Despite these studies, reports about the combined effects of multi-factors on N_2 fixation along steep geochemical gradients in hydrothermal systems are scarce.

Shallow submarine hydrothermal systems (SHSs) are defined as those occurring in less than 200 m of seawater [17]. Few N_2 fixation-related studies have been carried out there before. Besides steep geochemical gradients, an outstanding characteristic of SHS is the existence of sunlight, which can be used as the energy source of cyanobacterial diazotrophs, the most important marine N_2 fixers currently known. Therefore, SHS might develop a unique diazotrophic community structure and N_2 fixation pattern compared with DHS. Meanwhile, the complicated formation of vent fluids (meteoric water and groundwater, besides seawater, can also be important components of the vent fluids in SHSs) [17,18] and the combined influence of natural and anthropogenic processes [19] create a great variety of chemical conditions in SHSs, making them the ideal sites for studying N_2 fixation under the influence of multiple steep geochemistry gradients in hydrothermal systems. Here, we analyzed size-fractioned diazotrophic community compositions by high-throughput sequencing of the *nifH* gene along geochemistry gradients in two different hydrothermal vents of the SHS off Kueishantao Islet, Taiwan, and obtained the most comprehensive to-date information on diazotrophic phylogenetic diversity in hydrothermal ecosystems. Meanwhile, $^{15}N_2$-traced NFRs, ^{13}C-traced carbon fixation rates (CFRs), nitrogen nutrient concentrations, and other biogeochemical parameters were also measured to further understand the diazotrophic activity and potential contribution to total bioavailable nitrogen in response to steep geochemical gradients.

2. Materials and methods

2.1. Study sites and sampling

Samples were collected from two types of hydrothermal vents, white vent (WV) (24.83ºN, 121.96ºE) and yellow vent (YV) (24.84ºN, 121.96ºE), within a cluster of shallow hydrothermal vents off Kueishantao Islet along with a reference site (24.83ºN, 121.96ºE) in May and June 2019. The necessary permits had been obtained for sampling there. The water samples for *nifH* genetic diversity, NFR, CFR, and geochemical parameters measurements were collected at the white and yellow hydrothermal vent sites along a depth gradient from the inside of the vent, the bottom layer near the vent, the middle layer, and the surface layer. A reference site outside of the vents was also sampled from the bottom, middle, and surface layers. All water samples were collected directly by scuba divers using sterile pre-evacuated glass bottles. Detailed sampling information is shown in Table S1.

2.2. Environmental DNA (eDNA) extraction, nifH gene sequencing, and analysis

Two to four liters of seawater was filtered through 3 μm- and 0.22 μm-pore-size polycarbonate membranes (47 mm, Millipore, USA) in sequence, then the membranes were stored in –80 °C until eDNA extraction. The eDNA was extracted using the phenol-chloroform-isoamyl alcohol method as described by Massana et al. [20] with minor modifications. Extraction blanks were obtained by extracting triplicate membranes onto which pure water was filtered. The concentration of eDNA was measured using the Qubit dsDNA HS assay kit (Invitrogen, Life Technologies). A 359-bp region of *nifH* genes was amplified with a two-step nested polymerase chain reaction (PCR) strategy [21]. The first round of PCR contained 25 μL of Premix Ex Taq (Takara BioInc.), 1 μL of the primers nifH3 and nifH4 (100 μmol L^{-1}), 22 μL of double-distilled H_2O, and 1 μL of DNA template. This reaction was programmed as denaturation at 95 °C for 5 min, followed by 31 cycles of denaturation at 95 °C for 1 min, annealing at 57 °C for 1 min, and elongation at 72 °C for 1 min, with a final extension at 72 °C for 10 min. One microliter of PCR product from the first reaction was used as the DNA template for the second round of PCR with primers nifH1 and nifH2 (100 μmol L^{-1}). These primers contained a sequencing primer binding region, dual-index barcodes, and Illumina linkers (Table S2). The components and thermocycling conditions of the second round of PCR were the same as that of the first round of PCR, with the exception of an annealing temperature of 54 °C. Triplicate PCR products were checked by gel electrophoresis, pooled, purified using a Qiagen gel extraction kit (Qiagen Inc.), and quantified as described above. No PCR products were obtained from the extraction blanks.

Paired-end sequencing (2 × 250) was performed using the Illumina HiSeq2500 platform with Rapid Run Mode and Dual Flow Cell. All 18 samples were sequenced within a lane, generating between 80–165 thousand raw reads for each sample.

Quality control was performed using iTools Fqtools fqcheck (BGI Inc.), cutadapt (v 1.16), and readfq (v.8) to remove sequencing adapters and reads with ambiguous, low complexity (>10 consecutive same bases), and low quality (average score <30). This generated approximately 680 thousand clean reads in total. More than 99% of the clean paired reads were merged into single sequences using FLASH [22], after which the primer sequences were removed. Operational taxonomic units (OTUs) were clustered at 97% nucleotide sequence similarity using USEARCH (v7.0.1090), and chimeras were checked for and removed [23]. To compare OTU diversity among samples, the sequences were normalized to 20,449 sequences per sample. A maximum-likelihood phylogenetic tree of translated OTU representative sequences was constructed using MEGA7. The Jones–Taylor–Thornton (JTT) substitution model was used, with a bootstrap value of 1000. The OTU representative sequences were first classified using the National Center for Biotechnology Information nonredundant database with the BLAST program. The top 10 hit sequences (with e-value < 10^{-15}, identity > 97%, and coverage > 100 bp) for each query sequence were then evaluated manually to obtain the most optimal classification results. Sequences with greater than 95% amino acid identity (e-value < 10^{-15}, coverage > 80%) to any available NifH sequences belonging to major iron or sulfur-metabolism related groups (Chlorobi, Geobacteraceae, Desulfuromonadales, Desulfobacterales, Ferribacterium, Desulfovibrionales, Ectothiorhodospiraceae, and Chromatiaceae) in GeneBank were identified as iron or sulfur-metabolism related sequences. These results were further manually checked based on the topology information of the phylogenetic tree. All raw sequences from this study are deposited in the Sequence Read Archive (BioProject ID: PRJNA846180).

To compare the diazotrophic community composition in the Kueishantao SHS (KSHS) with those in other geothermal systems, *nifH* sequences retrieved from TGSs and DHSs were collected from previous studies (Table S3). These sequences were clustered into OTUs at 97% nucleotide sequence similarity using Mothur software [24]. Maximum-likelihood phylogenetic trees were constructed in MEGA7 based on translated OTU representative sequences, using the JTT substitution model and a bootstrap value of 1000. The similarities between OTU representative sequences from different habitats were calculated using the BLASTn program.

2.3. Amino acid composition and protein structure

The relative abundance of each amino acid in NifH sequences was obtained by dividing the number of occurrences of each amino acid by the protein length. To infer the conserved positions and structural domains in NifH fragments, sequence logos were drawn based on aligned amino acid sequences using the ggseqlogo package [25] in R. The protein structure of NifH fragments was predicted using ColabFold [26]. Protein structure alignment was performed and visualized using PyMOL (v2.5.2).

2.4. Biogeochemical parameters measurements

The biogeochemical parameters measurements were generally performed following the report by Zhang et al. [27]. The salinity was determined by converting the conductivity measurements taken from a Guildline salinometer (Autosal 8400B, Canada), while the *in-situ* temperatures were directly measured by scuba divers using a thermocouple. The pH values were determined at 25 ± 0.05 °C using a pH meter (Radiometer PHM-85, Denmark) calibrated with NIST Tris buffer. Dissolved oxygen (DO) was measured by spectrophotometry with a detection limit and precision of about 0.5 μM and 0.3%, respectively [28]. The NH_4^+ concentrations were measured using the indophenol method with a detection limit and precision of about 0.05 μM and 2.7%, respectively [29], with a HACH DR/890 colorimeter. The NO_3^- and NO_2^- concentrations were determined using the pink azo dye method by a flow injection analyzer. The samples for measuring chlorophyll *a* (Chl. *a*) concentration were extracted with 90% acetone from a 0.45 μm pore size Millipore filter. The Chl. *a* concentration was then determined using a Turner Designs model 10-AU fluorometer [30]. Silica (SiO_2) concentration was measured using the silicomolybdenum blue method with a flow injection analyzer [31]. Sulfide (S^{2-}) concentration was measured using the methylene blue method with a HACH DR/890 colorimeter. Sulfate (SO_4^{2-}) concentration was measured using ion chromatography. Dissolved CH_4 was measured using gas chromatography through the gas-stripping method [32]. Dissolved inorganic carbon (DIC) was determined using a Dissolved Inorganic Analyzer (Model AS-C3), with a precision of 0.1%. The accuracy was assessed using CO_2 certified reference materials. Dissolved organic carbon (DOC) was measured using a high TOCII analyzer (Elementar, Germany), using the method of high-temperature catalytic oxidation following the removal of inorganic carbon by acidification and oxygen purging. The accuracy was assessed using Low Carbon Water and Deep Sea Water.

2.5. NFRs and CFRs measurements

The measurement of NFRs was performed using the $^{15}N_2$ gas dissolution method [33,34]. First, 0.2 μm-filtered seawater was degassed as described in Shiozaki et al. [35]. Then 500 mL degassed seawater was transferred into an acid-cleaned, gas-tight plastic bag with no headspace, and 5 mL of 98% pure $^{15}N_2$ gas (Cambridge Isotope Laboratories) was injected into this bag to dissolve it in the seawater completely. The percentage of $^{15}N_2$ in the $^{15}N_2$-enriched seawater was validated using a gas chromatography isotope ratio mass spectrometry (IRMS; Thermo Fisher Delta V Plus).

The *in situ* seawater was collected and 0.4 L of which was filtered (<100 mm Hg) immediately onto pre-combusted (450 °C, 4 h) 25-mm diameter 0.3 μm pore-size glass fiber filters and stored at –20 °C for determining initial isotopic abundance. Residual seawater was filled in triplicate acid-cleaned 2.3 L polycarbonate bottles, in which the $^{15}N_2$-enriched water was added at approximately 2.6% of the total sample

volume and the $NaH^{13}CO_3$ (99 atom % ^{13}C, Cambridge Isotope Laboratories) solution was added at a final tracer concentration of 100 μM. Then the bottles were sealed and shaken at least five times before incubation. Incubation was performed in flow-through deck-board incubators under natural sea-surface irradiance (for samples from the surface and middle layer seawater) or the irradiance weaken by neutral-density plastic screens (for samples from the vent and bottom water) for 24 h. After incubation, water samples were also gently filtered onto pre-combusted (450 °C, 4 h) 25-mm diameter 0.3 μm pore-size glass fiber filters and immediately stored at –20 °C.

For determining ^{15}N and ^{13}C abundance, filters were firstly acid fumed to remove the inorganic carbon, then the concentrations and isotopic values of particulate organic nitrogen and particulate organic carbon were measured using a Flash elemental analyzer (Thermo Fisher Flash HT 2000) coupled to an IRMS (Thermo Fisher Delta V Plus). The NFRs and CFRs were calculated according to Mohr et al. [33] and Hama et al. [36], respectively. The detection limit for NFRs was estimated by taking 4‰ as the minimum acceptable change in the $\delta^{15}N$ of particulate nitrogen [37].

2.6. Statistical analysis

The Pearson correlation coefficients among OTUs, NFRs, CFRs, and biogeochemical parameters were calculated in *R*. The pheatmap package in R was utilized to perform hierarchical clustering of correlation coefficients between relative abundance of OTUs and biogeochemical parameters, NFR, and CFR based on Euclidean distances. Dissimilarity matrices were constructed based on Euclidean distances for biogeochemical parameters and Bray-Curtis distances for diazotrophic communities between samples. These matrices were used to determine correlations between biogeochemical parameters and diazotrophic community compositions. Mantel tests were then performed in *R*, and after 999 permutations, a significant factor was obtained based on Spearman correlations. Alpha diversity indices were calculated using the vegan package in *R*. The univariate linear regression analysis of NFRs on alpha diversities of different diazotrophic communities was performed and visualized in SigmaPlot 14.0. The differences in relative abundances of amino acids between NifH fragments from different sample sets were tested using the nonparametric Wilcoxon tests.

3. Results and discussion

3.1. Diazotrophic community compositions in the KSHS

Nine hundred and twenty OTUs of *nifH* sequences were recovered in this study and covered all four known *nifH* clusters (I, II, III, and IV) described by Zehr et al. [8] (Fig. 1). Among them, 769 OTUs were retrieved, 560 of which were unique, from the KSHS samples, while only 360 OTUs were retrieved from the reference site samples,

indicating a much higher diversity of *nifH* in the KSHS. Moreover, the number of OTUs from the KSHS was also much higher than those recovered from open ocean environments in previous studies using similar high-throughput sequencing methods [38,39,40]. The majority of the OTUs from the KSHS (677 OTUs, accounting for 88% of total OTUs) may be considered as novel species due to their nucleotide identity (NI) being less than 97% when compared to any sequence in GeneBank. The remaining OTUs (92 OTUs, or 12%) were closely related (>97% NI) to published sequences obtained from various environments from land to shore and the open ocean, including seawater, marine sediment, soil, groundwater, and biological tissue (Table S4). These findings reflect that the unique KSHS ecosystem, which harbors micro-environmental gradients, may contain a highly diverse and heterogeneous diazotrophic microbiota with many novel species likely to be undiscovered, as well as species sourced from both terrestrial and marine environments. Hierarchical clustering of communities based on OTUs indicated a general separation of diazotrophic communities in the vent and bottom water (VB) from those in other environments (the surface and middle layer water (SM) and the reference site) (Fig.1). Diverse proteobacteria groups within Cluster I along with the groups within Cluster III dominated diazotrophic communities in most samples. In the vent water of the WV site, the sequences belonging to Cluster III accounted for over 80% of total sequences, while in the vent and bottom water of the YV site, alpha- and beta-proteobacteria within Cluster I became the dominant diazotrophs (>65%) and the sequences belonging to Cluster III were hardly detected. In the SM, proteobacteria, including alpha-, beta- gamma-, and delta-proteobacteria, within Cluster I dominated the diazotrophic communities, while the relative abundances of groups within Cluster III were relatively lower. At the reference site, gamma-proteobacteria within Cluster I and the groups within Cluster III were the dominant diazotrophs in general.

We classified the OTUs into seven groups based on types of energy metabolism, including sulfur-oxidizing purple sulfur bacteria (PSB)-like and green sulfur bacteria (GSB)-like phylotypes, sulfate-reducing bacteria (SRB)-like phylotypes, iron-reducing bacteria (IRB)-like phylotypes, cyanobacteria, sulfur-oxidizing epsilon-proteobacteria, and other phylotypes, by blasting them against reference *nifH* sequences (Fig. 1). The VB of the YV site was primarily dominated by OTUs affiliated with IRB-like phylotypes, whereas the vent water of the WV site was dominated by OTUs affiliated with GSB-like and SRB-like phylotypes (Fig. 1). In contrast, the SM was dominated by PSB-like phylotypes and highly diverse other phylotypes that included many OTUs closely related to typical heterotrophic bacteria, such as Hyphomicrobiales, Sphingomonadales, Burkholderiales, and Pseudomonadales (88.2–93.5% NI). However, the widely distributed marine gamma-proteobacterial phylotype — Gamma A [41] was not recovered from the KSHS. Small amounts of phylotypes affiliated with sulfur-oxidizing epsilon-proteobacteria and cyanobacteria were also found in the VB (Fig. 1). It should be noted that the presence of *nifH* does not necessarily guarantee nitrogenase

functionality, as it can exist as an "orphan gene" [42]. Nevertheless, we obtained six metagenome-assembled genomes (MAGs) affiliated with potential N_2-fixing epsilon-proteobacteria using the published metagenome dataset from the same region (see Supplementary materials and Table S5). All of these MAGs belong to the order Campylobacterales and contain multiple nitrogenase subunit genes (*nifH*, *nifD*, and *nifK*), as well as sulfur-oxidation-related genes (*sox*) (Fig. S1), suggesting a potential coupling between N_2 fixation and sulfur oxidation for epsilon-proteobacterial diazotrophs within the KSHS ecosystem.

Diazotrophic phylogenetic compositions based on the *nifH* gene have been well described in TGSs [43–46] and DHSs [5,10,11]. We further compared the *nifH* phylotypes from these hydrothermal systems with those from the KSHS (Fig. 2). The phylotypes belonging to alpha/beta-, gamma-proteobacteria, and Cluster III were consistently found in all three environments. In TGSs, the unique phylum Aquificae and cyanobacteria account for the most of *nifH* phylotypes, while in DHSs, the groups affiliated with Cluster II and III contribute to the most of *nifH* phylotypes. The *nifH* phylogenetic compositions in the KSHS included some characteristics from both TGS and DHS. For example, cyanobacteria- and delta-proteobacteria-affiliated phylotypes that existed in TGSs and Cluster II-affiliated phylotypes that existed in DHSs were retrieved from the KSHS (Fig. 2). At the level of OTUs, the KSHS and TGSs shared some similar phylotypes (90%–97% NI) within proteobacteria (Fig. 2), the most similar phylotype (OTU822 and GQ426255.1 in [43], 96.7% NI) of which was closely related to Fe^{2+}-oxidizing acidophile strain *Acidithiobacillus ferriphilus* GT2 [47]. The OTUs similar to two alpha-proteobacteria-affiliated phylotypes (AY120669.1 [5] and KM109108.1 [11]) and one Cluster III-affiliated phylotype (AY120672.1 [5]) in the DHSs were also recovered from the KSHS (Fig. 2). However, no similar phylotypes (>90% NI) were found between the TGSs and DHSs (Fig. 2). These results suggest that the combining of physicochemical characteristics from TGSs (e.g. irradiation) and DHSs (e.g. salinity) in the SHS might develop diazotrophic groups adapted to terrestrial and deep-sea environments. Notably, 316 OTUs (most from Cluster III) of total 769 OTUs (41%) recovered from the KSHS had very low identities (<80% NI or <200 bp alignment length) with those in the TGSs and DHSs. So, besides physicochemical factors, geographic isolation may also be an important factor in shaping unique diazotrophic communities in the SHS.

3.2. Molecular adaptations of nitrogenase to SHS

The molecular characteristics of nitrogenase can more directly reflect the functional adaptation of diazotrophs to their environment, compared to community compositions. Translated *nifH* sequences from the VB with high temperature, extremely low pH, and high sulfur compound concentration (see next section for details) contained significantly higher proportions of glutamic acid residues and lower proportions of valine residues than those from the SM and the reference site (Wilcoxon tests, $P < 0.05$, Fig. 3a). This feature might help maintain the high thermal

stability of nitrogenase in the VB because a previous study has indicated that glutamic acid residues have a high positive correlation, while valine residues have a high negative correlation with the thermal stability of proteins [48]. Meanwhile, the excess of acidic glutamic acid surface residues on the enzyme might also be a strategy for it to adapt to the low pH conditions [49]. Notably, the high sulfur concentration in the VB did not result in the alteration of the proportion of sulfur-contained amino acid residues (methionine and cysteine) (Fig. 3a), implying that these residues were nonredundant and involved in conserved core functions. For instance, cysteines were key ligands to the Fe:S cluster which enabled electron transfer in nitrogenase iron protein [50].

The sequence logos revealed two conserved domains of the sequenced fragment of NifH (Fig. 3b). The two domains correspond to the residues 87 to 101 and residues 124 to 140 in the nitrogenase iron protein of *Azotobacter vinelandii*, and might be associated with the nucleotide-binding site, the Fe:S cluster, and the MoFe-protein-binding interface [51]. The high consistency of these core sites lends support to the theoretical activity of nitrogenase in the three niches (VB, SM, and reference site). Notably, for the sequences from the VB, additional 9–12 residues were found between the positions of 80 and 81 (Fig. 3b). All these additional residues are attributed to 12 OTUs affiliated with epsilon-proteobacteria that were exclusively recovered from the VB (Fig. 1). Similarly, a previous study also reported a longer NifH sequence in epsilon-proteobacteria compared with other diazotrophs [52]. Structure predictions for a representative epsilon-proteobacteria-affiliated sequence (OTU121) from the VB showed that its overall structure was still highly identical to that of NifH in *A. vinelandii*, although the additional residues formed a protruding coil away from the core domain (Fig. 3c). This suggests that these additional residues are unlikely to have a significant impact on the function of the enzyme. A previous study revealed the N_2 fixation activity of epsilon-proteobacteria from DHSs [53], and our results, which identified multiple nitrogenase subunit genes in the epsilon-proteobacterial MAGs, support the suggestion that they may be capable of performing N_2 fixation (Fig. S1). Such an additional proline-contained coil structure might be responsible for thermostability by reducing the backbone flexibility [54]. However, this structure was not found in some other known (hyper)thermophilic N_2 fixers, such as those affiliated with methanogenic archaea and Aquificae [6,15]. Horizontal gene transfer also could result in the change in the nitrogenase of epsilon-proteobacteria in hydrothermal environments [53].

Alternative nitrogenase (V- and Fe-only nitrogenase) may also play an important role in sulfide-rich environments alongside canonical Mo-nitrogenase due to low concentrations of Mo commonly found in waters of hydrothermal systems [16]. Indeed, many *nifH* sequences recovered from the SM and VB were closely related (88.4–99.4% NI) to those found in genomes containing nitrogenase gene *vnfD* or *anfD* (Table S6). These reference genomes are affiliated with diverse diazotrophic groups including filamentous cyanobacteria, nitrate-reducing bacteria, methane-oxidizing

bacteria, purple nonsulfur bacteria, and other typical heterotrophic bacteria. The similar occurrence frequencies of *vnfD* and *anfD* in these BLAST top hit genomes produced by the KSHS *nifH* sequences suggest that V and Fe were not limiting factors in this system (6–17 nmol L^{-1} and 15–108 nmol L^{-1}, respectively, based on a recent study [55]), despite the fact that V is known to easily precipitate in hydrothermal systems [56]. Riverine input may supplement the Mo and V levels in SHSs [57,58].

3.3. Environmental adaptations of active diazotrophs to SHS

Similar to the results of *nifH-harboring bacterial* community composition, the hierarchical clustering of biogeochemical parameters was also clearly separated into three clusters — the VB, SM, and the reference site clusters (Fig. 4a). The lowest temperature (25–26 °C) and CH_4 concentrations (103–1982 μmol L^{-1}) as well as the highest DO (91.5–93.8%), pH (7.9–8.1), Chl. *a* concentrations (0.07–0.13 μg L^{-1}), and NO_2^- concentrations (0.01–0.17 μmol L^{-1}) were found in the reference site; the lowest concentrations of NH_4^+ (2.4–9.2 μmol L^{-1}), NO_2^- (below detection limit (BD)), and NO_3^- (BD to 0.5 μmol L^{-1}) as well as the highest SO_4^{2-} concentrations (25.3–28.7 mmol L^{-1}) were found in the SM samples; the lowest pH (1.6–5.6), Chl. *a* concentrations (BD to 0.01 μg L^{-1}), and SO_4^{2-} concentrations (21.5–24.3 mmol L^{-1}) as well as the highest temperature (27–102 °C) and concentrations of SiO_2 (215–796 μmol L^{-1}), CH_4 (2874–10065 μmol L^{-1}), NH_4^+ (28.6–61.9 μmol L^{-1}), NO_3^- (BD to 28.2 μmol L^{-1}), and S^{2-} (1063–4250 μmol L^{-1}) were found in the VB samples (Fig. 4a).

The NFRs (9.7–28.7 nmol N $L^{-1}d^{-1}$) detected in the SM were among the highest values in the global ocean [59] (Fig. 4a), while relatively lower NFRs were detected for the reference site (1.9–6.9 nmol N $L^{-1}d^{-1}$) and VB samples (BD to 7.0 nmol N $L^{-1}d^{-1}$). In contrast, the CFRs in the SM (0.4–2.0 μmol C $L^{-1}d^{-1}$) were generally lower than those in the reference site (2.3–4.2 μmol C $L^{-1}d^{-1}$) and VB (up to 4.5 μmol C $L^{-1}d^{-1}$). This may be because low concentrations of inorganic nitrogen stimulated diazotrophic NFR but limited phytoplanktonic CFR in the SM (Fig. 4a), which was supported by the observed negative (and positive) correlations between the NFR (and CFR) and concentrations of NH_4^+, NO_2^-, and NO_3^- (Fig. 4b). In addition, the NFR was slightly positively correlated with pH and the concentrations of SO_4^{2-} and CH_4, and was negatively correlated with DO, temperature, salinity, and concentrations of DIC, SiO_2, and S^{2-} (Fig. 4b). These results are basically consistent with the previous findings regarding the influence of biogeochemical factors on nitrogenase activity and N_2-fixation reaction kinetics, e.g., N_2 fixation activity can be inhibited by low pH or high concentrations of oxygen and nitrogen compounds [13,60,61]. The enrichment of inorganic nitrogen around vents has also been reported in many deep-sea hydrothermal fluids [4,62,63], especially for NH_4^+, which can fuel the chemoautotrophic carbon fixation of nitrifiers [62]. Thus, the role of nitrogenase in the high NH_4^+ vent water needed to be further studied. One speculation is that these nitrogenases performed functions other than N_2 fixation; for example, they might serve to detoxify toxic chemicals such as cyanides which could exist in SHS [64,65].

In addition to nitrogen compounds, Fe is clearly another key factor controlling NFRs. A separate study from the same sampling sites reported high concentrations of Fe in the water above hydrothermal vents (up to 71.8 nmol L^{-1}) [55]. Based on the relatively low concentration of NO_x^- in the SM (Fig. 4a), the Fe to NO_x^--N supply ratio was estimated to be >0.15. According to data from the North Pacific, Fe:N supply ratios >0.1 were associated with high NFRs (5–10 nmol N L^{-1} d^{-1}) [66], which is similar to that observed in the SM (Fig. 4a). Therefore, the high Fe:N supply ratio may have promoted active N_2 fixation in the SM.

In addition, the differences in diazotrophic community compositions induced by varied environmental factors (Fig. 4c and d) can also contribute to the variation of NFRs due to the different N_2 fixation efficiencies/activities among taxa [67]. We found indeed that the alpha diversities of the diazotrophic communities (both total community and most abundant sub-groups) were positively correlated with the bulk NFRs, especially for the 0.2–3 μm size-fractional communities (Fig. S2). For example, the highest diazotrophic diversity was found in the SM where the NFRs were also the highest (Fig. S2). This phenomenon contradicted previous research in the open ocean where the hotspots (e.g., the Western Tropical Pacific and the Western North Atlantic) of N_2 fixation were usually dominated by few diazotrophic cyanobacterial phylotypes [68,69], while low-NFRs regions (e.g., the Eastern Tropical South Pacific (ETSP) and the South Pacific Gyre (SPG)) were dominated by highly diverse heterotrophic diazotrophs [67,70]. A possible explanation for such a contradiction was that the typical marine diazotrophic cyanobacteria (primarily resulting in the low diversity in the open ocean) were inhibited in the SHS due to their high sensitivity to toxic sulfide [71]. Thus, the coherence between the highly diverse non-cyanobacterial diazotrophic phylotypes and high bulk NFRs was observed in the SHS.

To better understand the niche characteristics of diverse diazotrophs and their potential contribution to N_2 or CO_2 fixation, we examined the correlations between the relative abundance of *nifH* OTUs and environmental parameters, as well as NFR and CFR (Fig. 5). Hierarchical clustering of correlation coefficients identified seven major OTU groups. Group 1 contained highly diverse OTUs belonging to Cluster III and proteobacteria within Cluster I, most of which (92%) were recovered from the 0.2–3 μm size fraction of the SM (Fig. 5). The relative abundances of these OTUs exhibited a significantly positive correlation with NFRs in general (Pearson correlation test, average p-value = 0.01). This suggests that these phylotypes were major contributors to N_2 fixation despite none having an average relative abundance of >2.5% in the SM. Only a small fraction of OTUs in Group 1 belonged to iron- and sulfur-metabolism-related phylotypes (Fig. 5), indicating that other phylotypes such as typical heterotrophic bacteria may play a key role in N_2 fixation. For example, OTU16, 18, 24, 25, and 34, which were among the most abundant OTUs within Group 1, were closely related to the sequences belonging to heterotrophic genera such as *Paraburkholderia*, *Bradyrhizobium*, *Azotobacter*, or unknown phylotypes. The contribution of heterotrophic bacteria to marine N_2 fixation has long been considered

negligible due to their extremely low cell-specific NFRs based on culture experiments [67] and low *in-situ* NFRs measured in heterotrophic diazotrophs-dominated oceanic regions (e.g., the ETSP and SPG) [72]. Recently published data indicated that microbial abundance in the SHS off Kueishantao Islet was as high as 4×10^9 L^{-1} [73], making it possible for the high diazotrophic abundance (usually 0.1–1% of total community [74]) to have led to the high bulk NFRs despite the putative low heterotrophic bacterial cell-specific NFRs (maximum of 10^{-4} nmol N $cell^{-1}$ d^{-1}) [67]. Moreover, favorable conditions for N_2 fixation in the SM (N-depleted, Fe-rich, and energy-rich) may greatly increase the diazotrophic abundance and activity. A previous study reported that active N_2 fixers accounted for 15%–20% of the microbial community in a sulfidic lake (Cadagno) with physio-chemical conditions similar to those of the SHS [75]. It was also possible that potential PCR bias had caused an underestimation of the roles played by PSB, SRB, and IRB in N_2 fixation [67]. However, the deficiency of S^{2-} in the SM (below detection limit; Fig. 4a) may have acted as a strong disincentive for sulfur-oxidizing PSB to perform N_2 fixation. Additionally, since SRB and IRB are mostly strictly anaerobic, their activities would be largely restricted in the generally oxygenated water in the SM (Fig. 4a). Thus, heterotrophic bacteria could be the primary candidate for performing high N_2 fixation in the SM. However, it remains unclear how heterotrophs overcome the sensitivity of nitrogenase to oxygen. It was possible that the spatial separation of oxygen from the cytoplasm and the respiratory protection within cells enabled the N_2 fixation of aerobic prokaryotes [76,77]. Furthermore, the anaerobic microenvironment in particles can also allow N_2 fixation to occur [78]. About 25% of OTUs in Group 1 were recovered from the >3 μm size fraction of the SM (Fig. 5), with most of them (56%) affiliated with unknown gamma-proteobacterial phylotypes, suggesting an important role of particle-associated gamma-proteobacterial diazotrophs in N_2 fixation within the SHS. Previous studies have reported dominant gamma-proteobacterial diazotrophs on sinking particles in the North Pacific Subtropical Gyre [79] and that the most widespread and well-studied marine gamma-proteobacterial *nifH* phylotype—Gamma A was also associated with particles [80].

Furthermore, Group 5 may represent a cluster of diazotrophs adapted to hydrothermal vents, exhibiting an overall significantly positive correlation with concentrations of NH_4^+ (p-value < 0.05 for 69% of OTUs), S^{2-} (p-value < 0.05 for 71% of OTUs), and CH_4 (p-value < 0.05 for 88% of OTUs). Most of OTUs within Group 5 (87%) were recovered from the 0.2–3 μm size fraction of the VB (Fig. 5), and this group contained abundant potential chemotrophic sulfur-oxidizing phylotypes within GSB and epsilon-proteobacteria (Fig. 5). However, these phylotypes may rarely contribute to local bulk N_2 fixation given no significantly positive correlation was found between them and NFRs (Fig. 5). A previous study in Lake Cadagno also indicated that GSB could be minor diazotrophs in low-sulfate and high-sulfide environments [75].

3.4. Perspective on N_2 fixation among potential nitrogen cycling processes of the KSHS

Collectively, extreme physicochemical conditions, such as high temperature, low pH, and toxic sulfide, can limit most typical diazotrophs that are adapted to temperate and oligotrophic oceans, resulting in a few chemotrophs as dominant N_2-fixers in the KSHS vents. Our analysis indicated that these chemotrophs showed potential molecular and metabolic adaptations to the extreme conditions. However, the role of these chemotrophic diazotrophs in the local N_2 fixation may be minor due to the abundant inorganic nitrogen compounds in the VB, leading to low NFRs there (Fig. 6). In contrast, the much lower concentrations of inorganic nitrogen in the SM than VB may stimulate N_2 fixation, leading to high NFRs there (Fig. 6). Such a drastic decay of inorganic nitrogen (mainly NH_4^+ and NO_3^-) from hydrothermal vent to ambient seawater probably owing to active ammonia oxidation, ammonia assimilation, denitrification, and anammox in hydrothermal vents [4,81,63]. In a previous study of the KSHS, metatranscriptomes retrieved the ammonia monooxygenase (*amoABC*) genes involved in ammonia oxidation [81]. The high nitrogen demand implied by the high CFR measured in the bottom water of this study suggested active NH_4^+ assimilation. Additionally, the low DO levels observed in the VB may facilitate the occurrence of anammox and denitrification (potentially coupled with sulfur oxidation under high S^{2-} concentration [82]) (Fig. 6). Based on the measurements from the same sampling sites [55], the high concentration of Fe in this SHS combined with low concentrations inorganic nitrogen in the SM leads to a high Fe:N supply ratio, which may promote active N_2 fixation in the SM. Our findings suggest that heterotrophic diazotrophs, rather than cyanobacterial diazotrophs, may play a dominant role in the N_2 fixation of the KSHS, potentially reshaping our understanding of marine heterotrophic diazotrophs. Over 50 active submarine hydrothermal vent fields have been identified globally [83], and a recent study reported that shallow submarine hydrothermal fluids can affect an area as large as 360,000 square kilometers [84]. Therefore, SHSs can be considered underexplored and vast reservoirs of potential nitrogen fixation.

4. Conclusion

This study reveals significant heterogeneity in diazotrophic communities and NFRs across sharply varying geochemical conditions, spanning from shallow submarine hydrothermal vents to ambient seawater. Furthermore, it sheds light on the molecular and metabolic adaptations of autochthonal diazotrophs, particularly epsilon-proteobacteria, to elevated temperatures and sulfur-enriched hydrothermal fluids. Bioavailable combined nitrogen and Fe are identified as key factors driving the formation of a pronounced contrast between the considerably elevated NFRs observed in seawater above the hydrothermal vents and the relatively low NFRs around the

vents. Notably, it is the diverse heterotrophic diazotrophs, rather than chemoautotrophic diazotroph, that are primarily responsible for N_2 fixation in the KSHS. This study suggests that the regions impacted by shallow water hydrothermal fluids may represent potential hotspots of marine N_2 fixation, urging us to reevaluate the global budget of nitrogen fixation in marine environments.

Declaration of competing interest

The authors declare that they have no conflicts of interest in this work.

Acknowledgments

This work was supported by grants from the NSFC projects (41721005 and 92251303) and Fujian Provincial Central Guided Local Science and Technology Development Special Project (2022L3078). We thank Dr. Zuozhu Wen and Prof. Shuh-Ji Kao for their advice in the sampling and measurements of NFRs.

Supplementary materials

Supplementary material associated with this article can be found in the online version.

References

[1] J.A. Baross, S.E. Hoffman, Submarine hydrothermal vents and associated gradient environments as sites for the origin and evolution of life, Origins of Life and Evolution of the Biosphere 15 (1985) 327-345.
[2] R.A. Zierenberg, M.W.W Adams, A.J. Arp, Life in extreme environments: Hydrothermal vents, Proceedings of the National Academy of Sciences 97 (2000) 12961-12962.
[3] K.S. Johnson, J.J. Childress, R.R. Hessler, et al., Chemical and biological interactions in the Rose Garden hydrothermal vent field, Galapagos spreading center, Deep Sea Research Part A. Oceanographic Research Papers 35 (1988) 1723-1744.
[4] P. Lam, J.P. Cowen, B.N. Popp, et al., Microbial ammonia oxidation and enhanced nitrogen cycling in the Endeavour hydrothermal plume, Geochimica et Cosmochimica Acta 72 (2008) 2268-2286.
[5] M.P. Mehta, D. A. Butterfield, J.A. Baross,. Phylogenetic diversity of nitrogenase (*nifH*) genes in deep-sea and hydrothermal vent environments of the Juan de Fuca Ridge, Applied and Environmental Microbiology 69 (2003) 960-970.
[6] M.P. Mehta, J.A. Baross, Nitrogen fixation at 92℃ by a hydrothermal vent archaeon, Science 314 (2006) 1783-1786.
[7] J.P. Zehr, L.A. Mcreynolds, Use of degenerate oligonucleotides for amplification of the *nifH* gene from the marine cyanobacterium Trichodesmium thiebautii, Applied and environmental microbiology 55 (1989) 2522-2526.
[8] J.P. Zehr, B.D. Jenkins, S.M. Short, et al. Nitrogenase gene diversity and microbial community structure: a cross-system comparison. Environmental microbiology 5

(2003) 539-554.
[9] M.P. Mehta, J.A. Huber, J.A. Baross, Incidence of novel and potentially archaeal nitrogenase genes in the deep Northeast Pacific Ocean, Environmental microbiology 7 (2005) 1525-1534.
[10] Y. Wu, Y. Cao, C. Wang, et al., Microbial community structure and nitrogenase gene diversity of sediment from a deep-sea hydrothermal vent field on the Southwest Indian Ridge, Acta Oceanologica Sinica 33 (2014) 94-104.
[11] H. Cao, Z. Shao, J. li, et al., Phylogenetic diversity of nitrogen-utilizing genes in hydrothermal chimneys from 3 middle ocean ridges, Extremophiles 19 (2015) 1173-1182.
[12] C.S. Fortunato, B. Larson, D.A. Butterfield, et al., Spatially distinct, temporally stable microbial populations mediate biogeochemical cycling at and below the seafloor in hydrothermal vent fluids, Environmental microbiology 20 (2018) 769-784.
[13] J.A. Sohm, E.A. Webb, D.G. Capone, Emerging patterns of marine nitrogen fixation, Nature Reviews Microbiology 9 (2011) 499-508.
[14] T.L. Hamilton, R.K. Lange, E.S. Boyd, et al., Biological nitrogen fixation in acidic high‐temperature geothermal springs in Yellowstone National Park, Wyoming, Environmental microbiology 13 (2011) 2204-2215.
[15] A. Nishihara, K. Matsuura, M. tank, et al., Nitrogenase activity in thermophilic chemolithoautotrophic bacteria in the phylum Aquificae isolated under nitrogen-fixing conditions from Nakabusa hot springs, Microbes and environments 33 (2018) 394-401.
[16] X. Zhang, D.M. Sigman, F.M.M. Morel, et al. Nitrogen isotope fractionation by alternative nitrogenases and past ocean anoxia, Proceedings of the National Academy of Sciences 111 (2014) 4782-4787.
[17] V.G. Tarasov, A.V. Gebruk, A.N. Mironov, et al., Deep-sea and shallow-water hydrothermal vent communities: two different phenomena?. Chemical Geology 224 (2005) 5-39.
[18] E. Valsami-Jones, E. Baltatzis, E.H. Bailey, et al., The geochemistry of fluids from an active shallow submarine hydrothermal system: Milos island, Hellenic Volcanic Arc, Journal of Volcanology and Geothermal Research 148 (2005) 130-151.
[19] R.E. Price, T. Pichler, Distribution, speciation and bioavailability of arsenic in a shallow-water submarine hydrothermal system, Tutum Bay, Ambitle Island, PNG, Chemical geology 224 (2005) 122-135.
[20] R. Massana, A.E. Murray, C.M. Preston, et al., Vertical distribution and phylogenetic characterization of marine planktonic Archaea in the Santa Barbara Channel, Applied and environmental microbiology 63 (1997) 50-56.
[21] J.P. Zehr, P. J. Turner, Nitrogen fixation: nitrogenase genes and gene expression, Methods in microbiology 30 (2001) 271-286.
[22] T. Magoč, S.L. Salzberg, FLASH: fast length adjustment of short reads to improve genome assemblies, Bioinformatics 27 (2011) 2957-2963.
[23] RC. Edgar, UPARSE: highly accurate OTU sequences from microbial amplicon

reads, Nature methods 10 (2013) 996-998.
[24] P.D. Schloss, S.L. Westcott, T. Ryabin, et al., Introducing mothur: open-source, platform-independent, community-supported software for describing and comparing microbial communities, Applied and environmental microbiology 75 (2009) 7537-7541.
[25] O. Wagih, ggseqlogo: a versatile R package for drawing sequence logos, Bioinformatics 33 (2017) 3645-3647.
[26] M. Mirdita, K. Schütze, Y. Moriwaki, et al. ColabFold: making protein folding accessible to all. Nature methods 19 (2022) 679-682.
[27] Y. Zhang, Z. Zhao, C.T.A. Chen, et al., Sulfur metabolizing microbes dominate microbial communities in andesite-hosted shallow-sea hydrothermal systems. PLoS ONE 7 (2012): e44593.
[28] S.C. Pai, G.C. Gong, K.K. Liu, Determination of dissolved oxygen in seawater by direct spectrophotometry of total iodine, Marine Chemistry 41 (1993) 343-351.
[29] Grasshoff, Klaus, Klaus Kremling, and Manfred Ehrhardt, Methods of seawater analysis, John Wiley & Sons, 2009.
[30] H. Naik, C.T.A. Chen, Biogeochemical cycling in the Taiwan Strait, Estuarine, Coastal and Shelf Science 78 (2008) 603-612.
[31] K.A. Fanning, M. Pilson. On the spectrophotometric determination of dissolved silica in natural waters, Analytical Chemistry 45 (1973) 136-140.
[32] J.W. Swinnerton, V. J. Linnenbom, Determination of the C1 to C4 hydrocarbons in sea water by gas chromatography, Journal of Chromatographic Science 5 (1967) 570-573.
[33] W. Mohr, T. Grosskopf, D.W.R. Wallace, et al., Methodological underestimation of oceanic nitrogen fixation rates, PloS one 5 (2010) e12583.
[34] Z. Wen, W. Lin, R. Shen, et al. Nitrogen fixation in two coastal upwelling regions of the Taiwan Strait, Scientific reports 7 (2017) 1-10.
[35] T. Shiozaki, T. Nagata, M. Ijichi, et al., Seasonal dynamics of nitrogen fixation and the diazotroph community in the temperate coastal region of the northwestern North Pacific, Biogeosciences Discussions 12 (2015) 865–889.
[36] T. Hama, T. Miyazaki, Y. Ogawa, et al., Measurement of photosynthetic production of a marine phytoplankton population using a stable 13C isotope, Marine Biology 73. (1983) 31-36.
[37] J.P. Montoya, M. Voss, P. Kahler, et al., A simple, high-precision, high-sensitivity tracer assay for N (inf2) fixation, Applied and environmental microbiology 62 (1996) 986-993.
[38] H. Farnelid, A.F. Andersson, S. Bertilsson, et al. Nitrogenase gene amplicons from global marine surface waters are dominated by genes of non-cyanobacteria, PloS one 6 (2011) e19223.
[39] P. Xiao, Y. Jiang, Y. Liu, et al., Re-evaluation of the diversity and distribution of diazotrophs in the South China Sea by pyrosequencing the *nifH* gene, Marine and Freshwater Research 66 (2015) 681-691.

[40] M.R. Gradoville, D. Bombar, B.C. Crump, et al., Diversity and activity of nitrogen‐fixing communities across ocean basins, Limnology and Oceanography 62 (2017) 1895-1909.
[41] R. Langlois, T. Großkopf, M. Mills, et al., 2015. Widespread distribution and expression of Gamma A (UMB), an uncultured, diazotrophic, γ-proteobacterial *nifH* phylotype, PloS one 10, e0128912.
[42] P.C. Dos Santos, Z. Fang, S.W. Mason, et al., Distribution of nitrogen fixation and nitrogenase-like sequences amongst microbial genomes, BMC genomics 13 (2012) 1-12.
[43] T.L. Hamilton, E.S. Boyd, J.W. Peters. Environmental constraints underpin the distribution and phylogenetic diversity of *nifH* in the Yellowstone geothermal complex, Microbial ecology 61 (2011) 860-870.
[44] J.R. Hall, K.R. Mitchell, O. Jackson-Weaver, et al., Molecular characterization of the diversity and distribution of a thermal spring microbial community by using rRNA and metabolic genes, Applied and environmental microbiology 74 (2008) 4910-4922.
[45] S.T. Loiacono, D.A.R. Meyer‐Dombard, J.R. Havig, et al., Evidence for high‐temperature in situ *nifH* transcription in an alkaline hot spring of Lower Geyser Basin, Yellowstone National Park, Environmental microbiology 4 (2012) 1272-1283.
[46] A. Nishihara, V. Thiel, K. Matsuura, et al., Phylogenetic diversity of nitrogenase reductase genes and possible nitrogen-fixing bacteria in thermophilic chemosynthetic microbial communities in Nakabusa hot springs, Microbes and environments 4 (2018) 357-365.
[47] M.S. Guzman, D. Reed, Y. Fujita, et al., 2022. Complete Genome Sequence of Acidithiobacillus ferriphilus GT2, isolated from gold mill tailings, Microbiology Resource Announcements 11, e01089-21.
[48] P.K. Ponnuswamy, R. Muthusamy, P. Manavalan, Amino acid composition and thermal stability of proteins, International Journal of Biological Macromolecules 4 (1982) 186-190.
[49] C.J. Reed, H. Lewis, E. Trejo, et al., 2013. Protein adaptations in archaeal extremophiles, Archaea 373275
[50] J.B. Howard, R. Davis, B. Moldenhauer, et al., Fe: S cluster ligands are the only cysteines required for nitrogenase Fe-protein activities, Journal of Biological Chemistry 264 (1989) 11270-11274.
[51] J.L. Schlessman, D. Woo, L. Joshua-Tor, et al., Conformational variability in structures of the nitrogenase iron proteins from Azotobacter vinelandii and Clostridium pasteurianum, Journal of molecular biology 280 (1998) 669-685.
[52] D. Man‐Aharonovich, N. Kress, E.B. Zeev, et al., Molecular ecology of *nifH* genes and transcripts in the eastern Mediterranean Sea, Environmental microbiology 9 (2007) 2354-2363.
[53] J.L. Meyer, J.A. Huber, Strain-level genomic variation in natural populations of Lebetimonas from an erupting deep-sea volcano, The ISME journal 8 (2014) 867-880.
[54] K. Watanabe, K. Chishiro, K. Kitamura, et al., Proline residues responsible for

thermostability occur with high frequency in the loop regions of an extremely thermostable oligo-1, 6-glucosidase from Bacillus thermoglucosidasius KP1006, Journal of Biological Chemistry 266 (1991) 24287-24294.
[55] K. Mei, D. Wang, Y. Jiang, et al., Transformation, fluxes and impacts of dissolved metals from shallow water hydrothermal vents on nearby ecosystem offshore of Kueishantao (NE Taiwan). Sustainability 14 (2022) 1754.
[56] F. Wu, J.D. Owens, C.R. German, et al. Vanadium isotope fractionation during hydrothermal sedimentation: implications for the vanadium cycle in the oceans, Geochimica et Cosmochimica Acta 328 (2022) 168-184.
[57] C. Archer, D. Vance, The isotopic signature of the global riverine molybdenum flux and anoxia in the ancient oceans, Nature Geoscience 1(2008) 597-600.
[58] S.G. Nielsen, Vanadium Isotopes: A Proxy for Ocean Oxygen Variations. Cambridge University Press, Cambridge, 2021.
[59] Y. Luo, S.C. Doney, L.A. Anderson, et al., Database of diazotrophs in global ocean: abundance, biomass and nitrogen fixation rates, Earth System Science Data 4 (2012) 47-73.
[60] R.L. Robson, J.R. Postgate, Oxygen and hydrogen in biological nitrogen fixation, Annual Reviews in Microbiology 34 (1980) 183-207.
[61] H.Z. Hong, R. Shen, F. Zhang, et al., The complex effects of ocean acidification on the prominent N2-fixing cyanobacterium Trichodesmium, Science 356 (2017) 527-531.
[62] P. Lam, J.P. Cowen, R.D. Jones, Autotrophic ammonia oxidation in a deep-sea hydrothermal plume, FEMS microbiology ecology 47 (2004) 191-206.
[63] A. Bourbonnais, M.F. Lehmann, D.A. Butterfield, et al., 2012. Subseafloor nitrogen transformations in diffuse hydrothermal vent fluids of the Juan de Fuca Ridge evidenced by the isotopic composition of nitrate and ammonium, Geochemistry, geophysics, geosystems 13, Q02T01.
[64] P.B. Rimmer, O. Shorttle, Origin of life's building blocks in carbon-and nitrogen-rich surface hydrothermal vents, Life 9 (2019) 12.
[65] W.S. Silver, J.R. Postgate, Evolution of asymbiotic nitrogen fixation, Journal of Theoretical Biology 40 (1973) 1-10.
[66] Z. Wen, T.J. Browning, Y. Cai, et al., Nutrient regulation of biological nitrogen fixation across the tropical western North Pacific, Science advances 8 (2022) eabl7564.
[67] K.A. Turk‐Kubo, M. Karamchandani, D.G. Capone, et al., The paradox of marine heterotrophic nitrogen fixation: abundances of heterotrophic diazotrophs do not account for nitrogen fixation rates in the Eastern Tropical South Pacific, Environmental microbiology 16 (2014) 3095-3114.
[68] H. Berthelot, M. Benavides, P.H. Moisander, et al., High‐nitrogen fixation rates in the particulate and dissolved pools in the Western Tropical Pacific (Solomon and Bismarck Seas), Geophysical Research Letters 44 (2017) 8414-8423.
[69] M.R. Mulholland, P.W. Bernhardt, B.N. Widner, et al., High rates of N_2 fixation

in temperate, western North Atlantic coastal waters expand the realm of marine diazotrophy, Global Biogeochemical Cycles 33 (2019) 826-840.
[70] H. Halm, P. Lam P, T.G. Ferdelman, et al., Heterotrophic organisms dominate nitrogen fixation in the South Pacific Gyre, The ISME journal 6 (2012) 1238-1249.
[71] Y. Cohen, B.B. Jørgensen, N.P. Revsbech, et al., Adaptation to hydrogen sulfide of oxygenic and anoxygenic photosynthesis among cyanobacteria, Applied and Environmental Microbiology 51 (1986) 398-407.
[72] S. Bonnet, M. Caffin, H. Berthelot, et al., Hot spot of N_2 fixation in the western tropical South Pacific pleads for a spatial decoupling between N_2 fixation and denitrification, Proceedings of the National Academy of Sciences 114 (2017) E2800-E2801.
[73] Y.S. Lin, H.T. Lin, B.S. Wang, et al., Intense but variable autotrophic activity in a rapidly flushed shallow‐water hydrothermal plume (Kueishantao Islet, Taiwan), Geobiology 19 (2021) 87-101.
[74] T.O. Delmont, J.J. Pierella Karlusich, I. Veseli, et al., Heterotrophic bacterial diazotrophs are more abundant than their cyanobacterial counterparts in metagenomes covering most of the sunlit ocean, The ISME Journal 16 (2022) 927-936.
[75] M. Philippi, K. Kitzinger K, J.S. Berg, et al., Purple sulfur bacteria fix N_2 via molybdenum-nitrogenase in a low molybdenum Proterozoic ocean analogue, Nature communications 12 (2021) 1-12.
[76] R.K. Poole, S. Hill, Respiratory protection of nitrogenase activity in Azotobacter vinelandii—roles of the terminal oxidases, Bioscience reports 17 (1997) 303-317.
[77] D. Tec-Campos, C. Zuñiga, A. Passi, et al., Modeling of nitrogen fixation and polymer production in the heterotrophic diazotroph Azotobacter vinelandii DJ, Metabolic engineering communications 11 (2020) e00132.
[78] J.P. Zehr, D.G. Capone. Changing perspectives in marine nitrogen fixation, Science 368 (2020): eaay9514.
[79] H. Farnelid, K. Turk-Kubo, H. Ploug, et al., Diverse diazotrophs are present on sinking particles in the North Pacific Subtropical Gyre, The ISME journal 13 (2019) 170-182.
[80] F.M. Cornejo-Castillo, J.P. Zehr, Intriguing size distribution of the uncultured and globally widespread marine non-cyanobacterial diazotroph Gamma-A, The ISME journal 15 (2020) 124-128.
[81] Y. Li, K. Tang, L. Zhang et al., 2018. Coupled carbon, sulfur, and nitrogen cycles mediated by microorganisms in the water column of a shallow-water hydrothermal ecosystem, Frontiers in microbiology 9, 2718.
[82] M.F. Shao, T. Zhang, H.H. Fang, Sulfur-driven autotrophic denitrification: diversity, biochemistry, and engineering applications, Applied microbiology and biotechnology 88 (2010) 1027-1042.
[83] S.E. Beaulieu, E.T. Baker, C.R. German, et al., An authoritative global database for active submarine hydrothermal vent fields, Geochemistry, Geophysics, Geosystems 14 (2013) 4892-4905.

[84] S. Bonnet, C. Guieu, V. Taillandier, et al., Natural iron fertilization by shallow hydrothermal sources fuels diazotroph blooms in the Ocean, Science 380 (2023) 812-817.

Figures

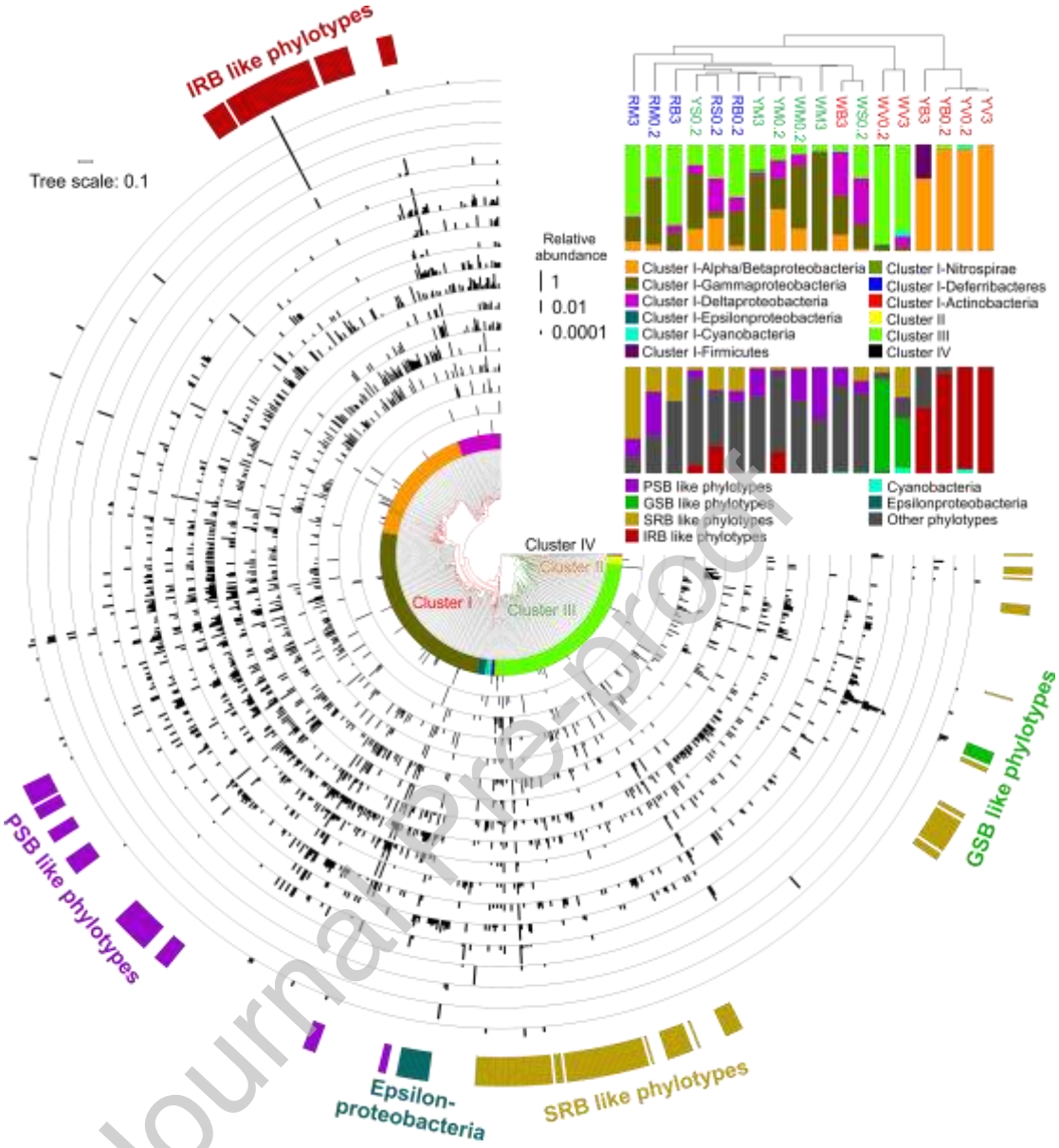

Fig. 1. Phylogenetic compositions of partial *nifH* sequences (OTUs) recovered from the shallow submarine hydrothermal system off Kueishantao (KSHS) and their distributions across different samples. Maximum-likelihood phylogenetic tree was built using translated *nifH* sequences in the center of this panel. The relative abundances of OTUs across different samples are shown with a histogram at the periphery of this tree, ordered by the result of hierarchical clustering of OTU compositions. The innermost colored arcs located near the tree, and the right upper scale bar chart indicate classical major diazotrophic groups according to Zehr et al. [8]. Below this chart, the scale bar chart indicates the *nifH* community composition categorized by types of energy metabolism. In addition, the OTUs related to major iron- and sulfur-metabolism are marked at the outermost edge of this panel. IRB, iron-reducing bacteria; GSB, green sulfur bacteria; PSB, purple sulfur bacteria; SRB, sulfate-reducing bacteria. Abbreviations indicating sample sources are as follows: "R

(reference site)/W (WV site)/Y (YV site)+S (surface water)/M (middle layer water)/B (bottom water)/V (vent water)+0.2 (0.2–3 μm size fraction)/3 (>3 μm size fraction)". Red, green, and blue colors indicate the vent and bottom water of KSHS, surface and middle layer water of KSHS, and reference site, respectively.

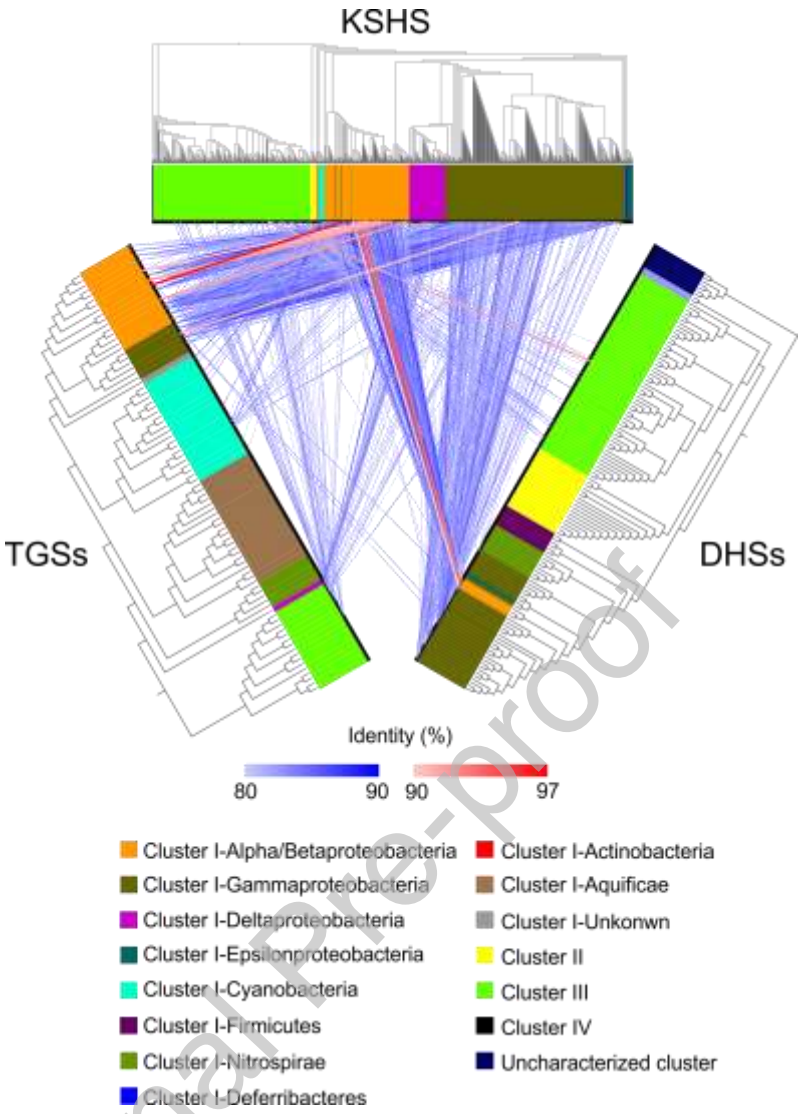

Fig. 2. Comparison of *nifH* phylogenetic compositions from the shallow submarine hydrothermal system off Kueishantao (KSHS, the upper panel), terrestrial geothermal systems (TGSs, the left panel), and deep-sea hydrothermal systems (DHSs, the right panel). Maximum-likelihood phylogenetic trees were built using translated OTU representative sequences. The OTUs from different niches with >80% nucleotide identity (NI) with each other are connected using lines, and the degree of NI is represented by different colors (see color bars).

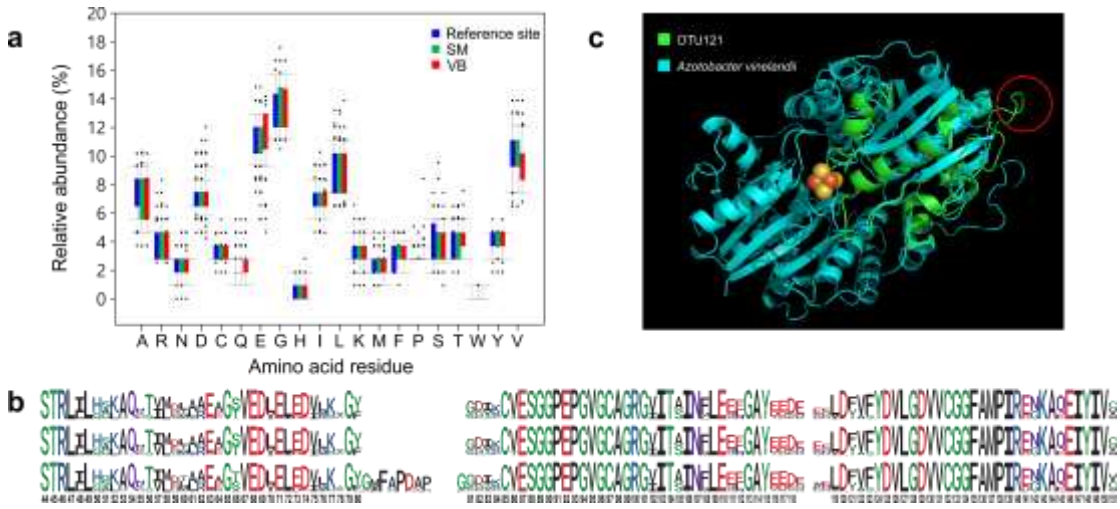

Fig. 3. Amino acid compositions and protein structure of NifH fragments recovered from the KSHS. (a) The relative abundance of each amino acid in translated OTU representative sequences recovered from the reference site, SM, and VB. (b) Sequence logos indicating amino acid compositions in each residue site of translated OTU representative sequences recovered from the reference site (upper), SM (middle), and VB (lower). The sequences logos are numbered according to the NifH sequence of *Azotobacter vinelandii*. (c) Structural comparison of the representative epsilon-proteobacterial NifH fragment (OTU121) from the KSHS and the NifH protein of *Azotobacter vinelandii*. The additional proline-contained coil structure is circled in red. Abbreviation for amino acid residues: A, Alanine; R, Arginine; N, Asparagine; D, Aspartic acid; C, Cystine; Q, Glutamine; E, Glutamic acid; G, Glycine; H, Histidine; I, Isoleucine; L, Leucine; K, Lysine; M, Methionine; F, Phenylalanine; P, Proline; S, Serine; T, Threonine; W, Tryptophan; Y, Tyrosine; V, Valine.

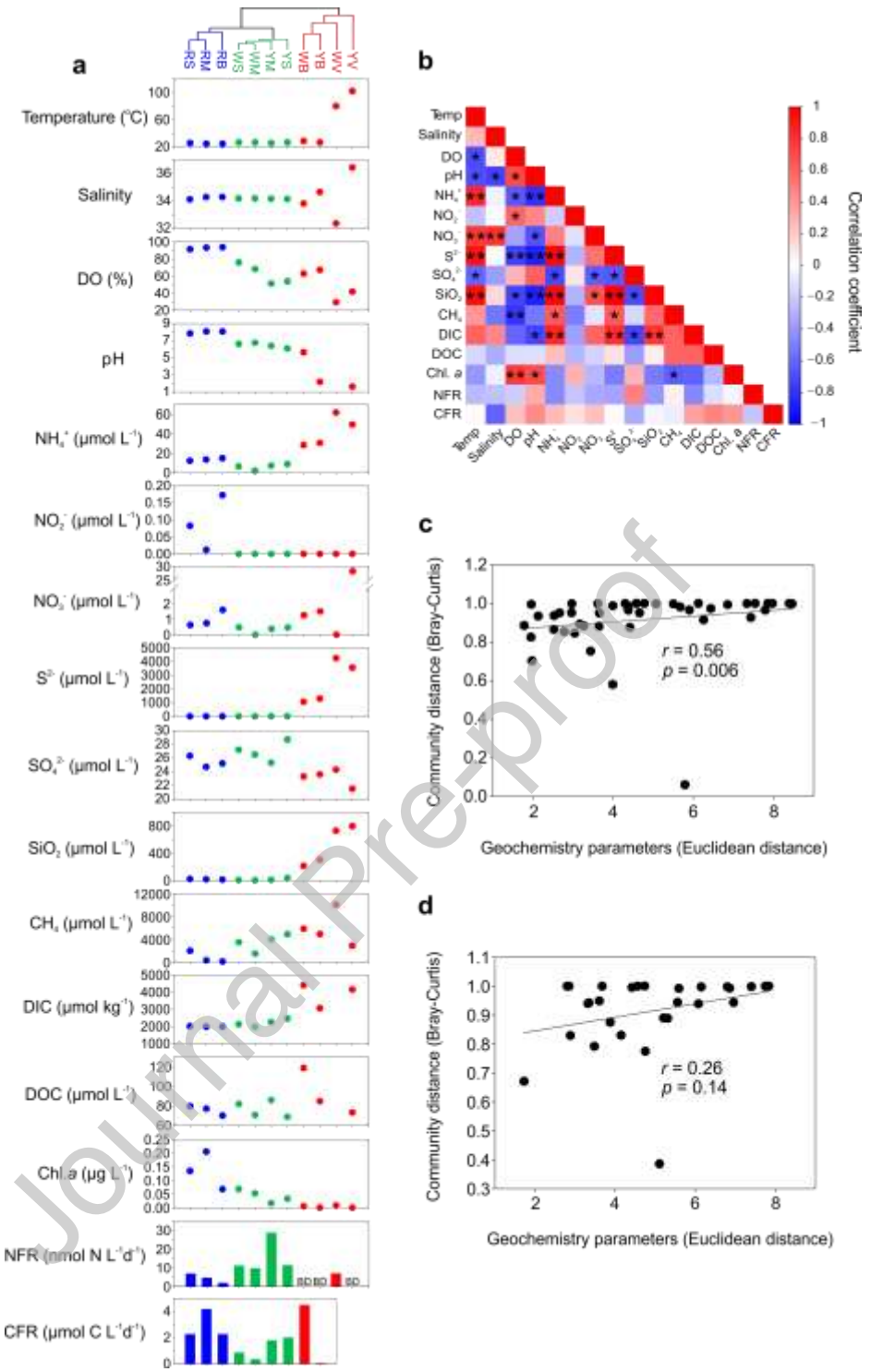

Fig. 4. Integrated analysis of biogeochemical parameters, N_2 and carbon fixation rates, and diazotrophic community composition. (a) Profiles of biogeochemical parameters, N_2 fixation rate (NFR), and carbon fixation rate (CFR) across different samples. (b) Pearson correlations among biogeochemical parameters, NFR, and CFR. (c) Spearman correlations between Euclidean distances of biogeochemical parameters and Bray–Curtis distances of OTUs-based communities in the 0.2–3 μm size fraction and (d) in the >3 μm size fraction. BD, below detection limit; *, $p < 0.05$; **, $p < 0.01$. Abbreviations indicating sample sources are "R (reference site)/W (WV site)/Y (YV

site)+S (surface water)/M (middle layer water)/B (bottom water)/V (vent water)". Temp, temperature; DO, dissolved oxygen; DIC, dissolved inorganic carbon; DOC, dissolved organic carbon; Chl. *a*, chlorophyll *a*.

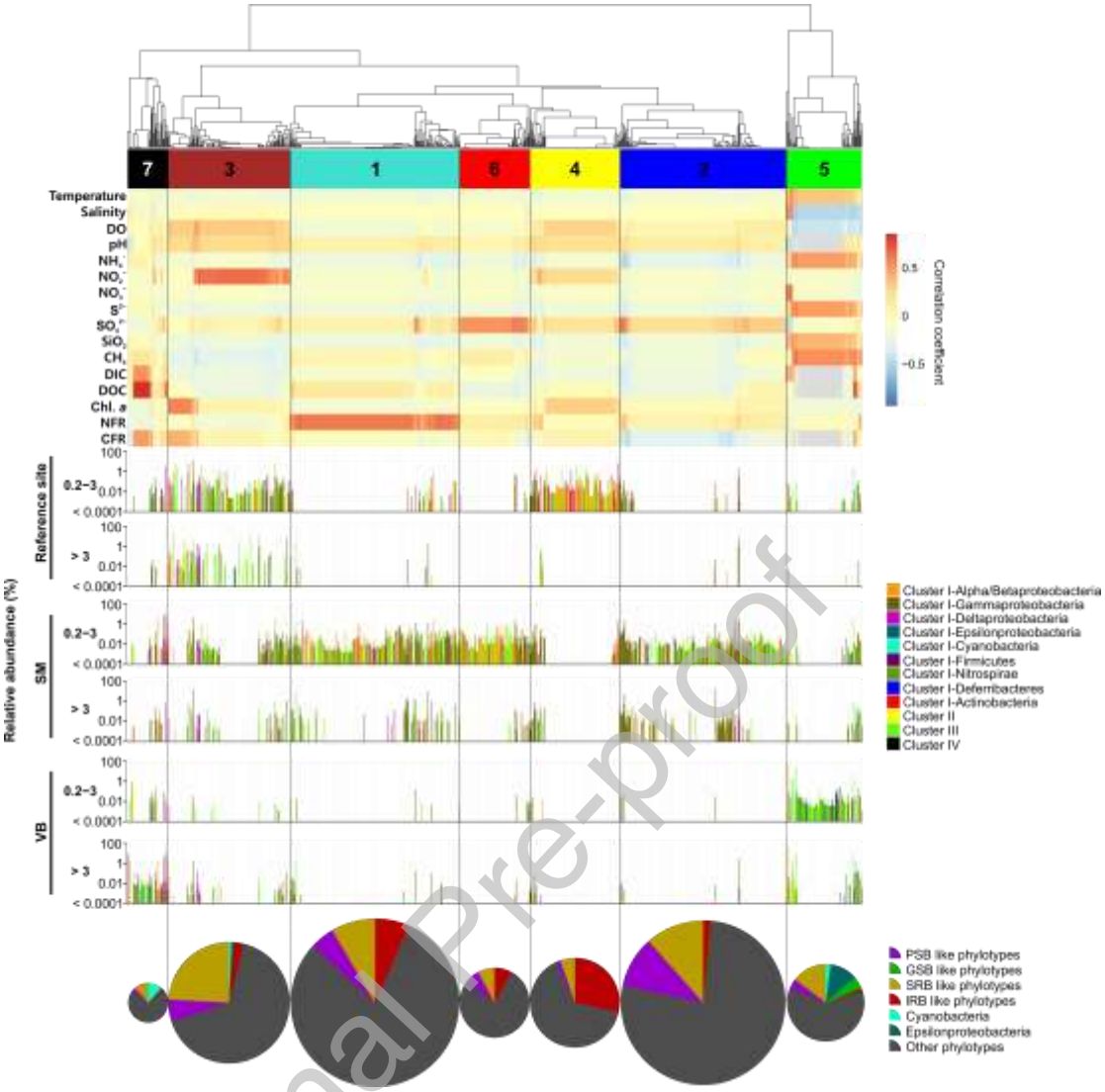

Fig. 5. Hierarchical clustering based on correlation coefficients between relative abundance of OTUs and biogeochemical parameters, N_2 fixation rate (NFR), and carbon fixation rate (CFR). The average relative abundance of each OTU in the 0.2–3 and >3 μm size fractions of the reference site, the surface and middle layer water (SM), and the vent and bottom water (VB) is shown in the histogram below the clustering heatmap; major diazotrophic clusters based on Zehr et al. [8] are distinguished with different colors as shown in the legend. The proportions of OTUs belonging to various important functional phylotypes in each clustering group are also shown in a pie chart; the size of each pie chart corresponds to the total number of OTUs. IRB, iron-reducing bacteria; GSB, green sulfur bacteria; PSB, purple sulfur bacteria; SRB, sulfate-reducing bacteria; DO, dissolved oxygen; DIC, dissolved inorganic carbon; DOC, dissolved organic carbon; Chl. *a*, chlorophyll *a*.

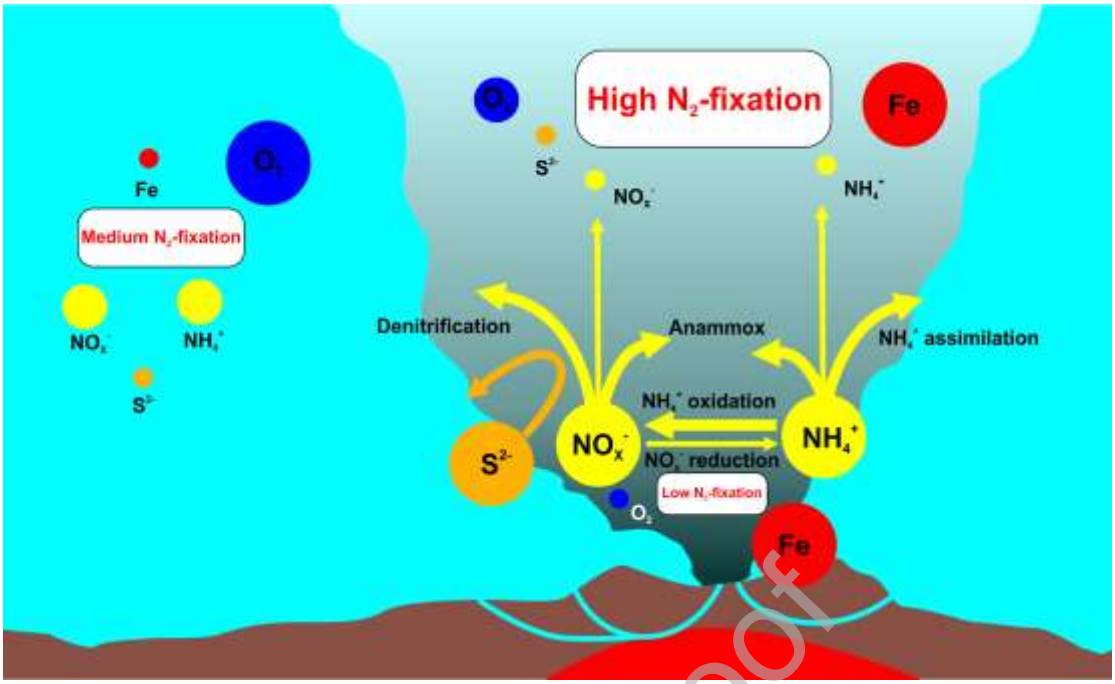

Fig. 6. Perspective on distribution pattern and biogeochemical control of N_2 fixation among potential nitrogen cycling processes in the KSHS. Inorganic nitrogen compounds (NO_x^- and NH_4^+), iron (Fe), sulfide (S^{2-}), and oxygen (O_2) are shown with yellow, red, orange, and blue circles, respectively. The sizes of circles reflect the concentration of each component in different niches of the KSHS. Arrows represent biogeochemical processes.

Mingming Chen received his B.S. degree in biotechnology and M.S. degree in marine biology from Ningbo University and Xiamen University in 2014 and 2018, respectively. After that, he worked as a research assistant for three years at Xiamen University (2018-2021). He is currently a Ph.D. candidate at the College of Ocean and Earth Sciences, Xiamen University. His research interests are marine nitrogen fixation processes and marine metagenomics.

Yao Zhang received her B.S., M.S., and Ph.D. degrees from Xiamen University. She worked as a post-doctoral fellow at Royal Netherlands Institute for Sea Research (NIOZ) (2007-2008) and as a visiting scholar at University of Delaware (2004) and University of Vienna (2014). She joined Xiamen University in 2006 and currently serves as a Nanqiang Chair Professor (2021-). Her research interests include microbial oceanography focusing on microbial processes involved in marine carbon/nitrogen biogeochemical cycles, microbial and molecular ecology with emphasis on structure and function relationships in microbial communities, and marine microbial evolution.

Graphical Abstract

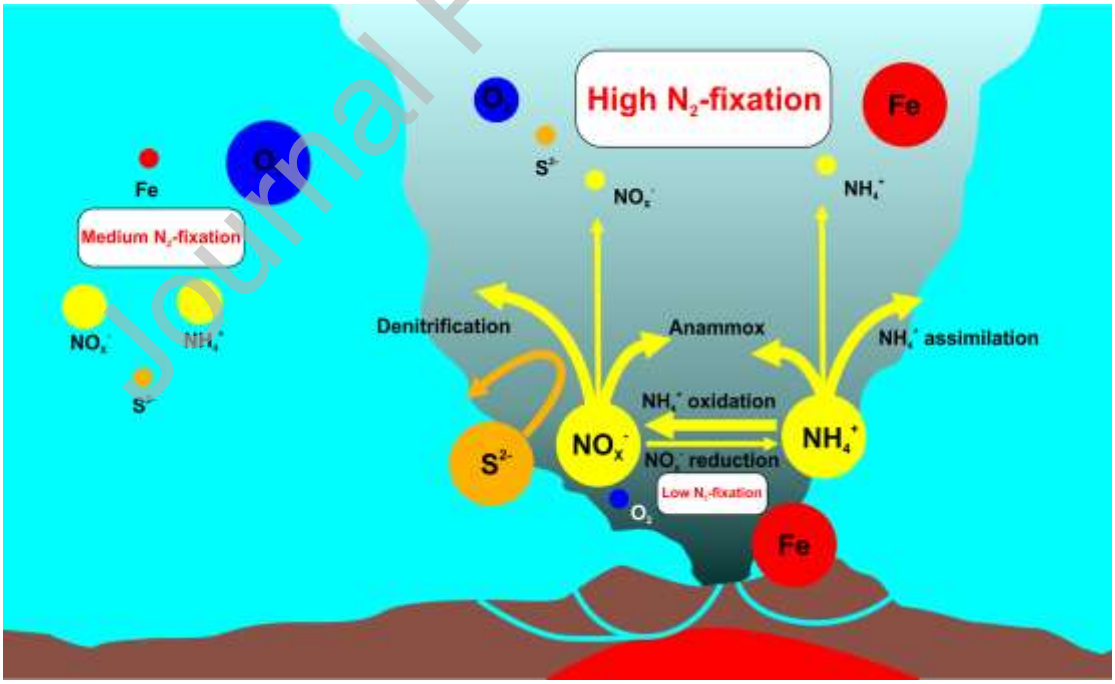

Declaration of interests

☒ The authors declare that they have no known competing financial interests or personal relationships that could have appeared to influence the work reported in this paper.

☐The authors declare the following financial interests/personal relationships which may be considered as potential competing interests: